Revival Structure of Aligned Rotational Wave Packets

Tamar Seideman*

Steacie Institute for Molecular Science, National Research Council of Canada, Ottawa, Ontario, Canada K1A 0R6

(Received 5 February 1999)

The revival structure of strong-field-induced rotational wave packets differs qualitatively from revival structures analyzed in the past. One of the consequences of this difference is strong enhancement of the alignment of such wave packets after turn-off of the laser pulse, under field-free conditions.

PACS numbers: 33.15.Bh, 33.80.–b, 42.50.Md

Rotational wave packets are broad, coherent superpositions of total angular momentum levels of molecules, created through multiple Rabi-type cycles in intense laser fields [1–3]. They have properties in common with angular wave packets of atomic Rydberg levels [4] and with molecular vibrational wave packets [5] but differ from both types of well-studied systems in their mode of preparation, applications, and most properties. The evolution of rotational wave packets during the laser pulse was explored in several recent theoretical [1,2] and experimental [3] studies. Their field-free evolution, subsequent to the laser pulse, was not analyzed as yet [6].

The analogous problem in the case of Rydberg [7] and vibrational [8] wave packets is well understood [9,10]. In general quantum mechanical superposition states dephase subsequent to initial evolution following a classical trajectory. If, however, the underlying classical dynamics is stable and periodic, the wave packet is reconstructed after a time T_{rev}, characteristic of the anharmonicity of the potential, and for a while evolves classically again [9,10]. Such wave-packet revivals were observed in Rydberg [7] and vibrational [8] wave packets as well as in one-atom masers and optical lattices. Below we show that the revival structure of rotational wave packets differs qualitatively from revival structures analyzed in the past, this difference carrying significant formal and practical implications.

General interest in rotational revivals arises for several reasons. First is the recent realization that rotational wave packets can, under very general conditions (*vide infra*), be induced to sharply align along a given direction in space. Molecular alignment has been one of the most important goals of modern reaction dynamics due to its role in stereodynamical and surface scattering research [11], surface catalysis [12], and surface processing [13]. Consequently, recent theoretical [1,2] and experimental [3] evidence that moderately intense lasers can induce sharp and controllable alignment raised considerable interest. The above applications, however, require that alignment be realized under field-free conditions. Second is the recognition that gas-phase short-pulse experiments are generally carried out under nonperturbative intensities [1,14]. Depending on the molecular mass, the intensity, and the pulse duration, different degrees of rotational excitation are likely to occur in many time-resolved experiments. Understanding of the long-time evolution of rotational superposition states is therefore relevant for the interpretation of most pump-probe studies, in particular, those that probe angular distributions or rotational spectra. Third are several unique features of rotational wave packets, illustrated below, which distinguish them from better-studied wave packets and make them an interesting model for analysis of revival structures.

Figure 1 shows a rotational wave packet vs time and the polar Euler angle θ during and after the laser pulse. The calculation was performed under the conditions used in the pump-probe experiment of Ref. [15] but at higher intensity. All vibrational levels accessed by the pulse are included in an exact quantum mechanical calculation and *ab initio* data are used for the potential energy surfaces and transition dipole elements. The remarkable feature of Fig. 1 is that the alignment is strongly enhanced *after* the laser pulse turn-off and further enhanced at long time. Qualitatively similar results were obtained under widely different field conditions, both near and far-off electronic resonance frequencies, and for other systems, including, in the near resonance case, both parallel and perpendicular transitions.

Part of the new phenomenon can be understood classically. Alignment enhancement is obtained in what could be termed a sudden excitation regime. A short (as compared to rotational periods) pulse imparts a "kick" to the molecule, which transfers to it angular momentum and sets it into angular motion in the direction of the kick once field-free. A familiar analog is the problem of Rydberg wave-packet ionization with half-cycle pulses [16], where a pulse of short duration as compared to the Kepler orbit rapidly transfers linear momentum to the electron, setting it into motion in the direction of the kick after the pulse is gone. Figure 1 suggests, however, that the enhancement effect is not merely a short time phenomenon that can be understood in classical terms. Rather, the alignment continues to improve through the long time, purely quantum mechanical stages of the evolution and is thus largely a quantum interference effect. Below we develop an analytical model that studies the early and late post-pulse evolution stages of intense-field-induced rotational wave packets and explains the observations of Fig. 1 and their generality.

0031-9007/99/83(24)/4971(4)$15.00

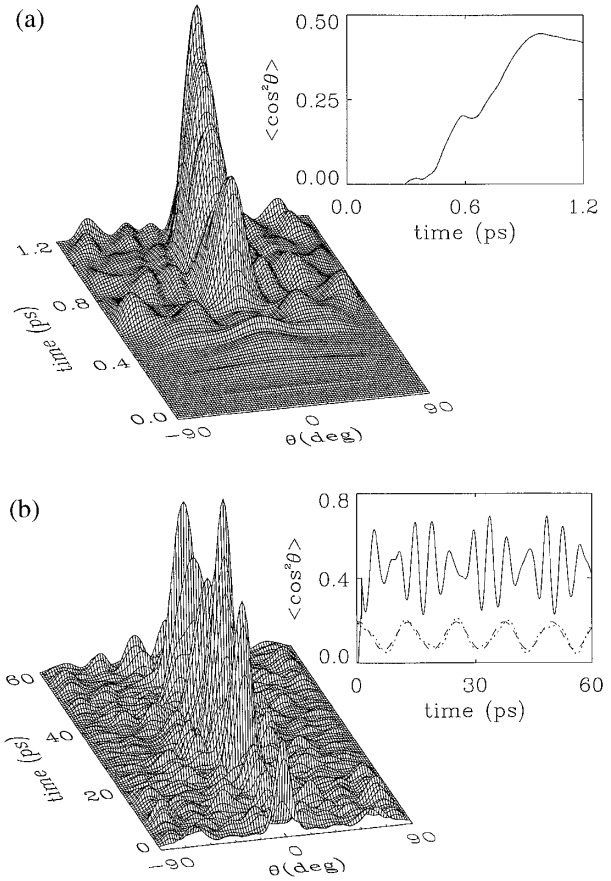

FIG. 1. The electronically excited component of a Li_2 rotational wave packet (a) during and (b) after a 10^{11} W cm^{-2}, 200 fs laser pulse centered at 600 fs and tuned near resonance with the $E \leftarrow A$ transition. The system is initially prepared in a single vibrational level with $J_i = 0$. The solid curves in the insets give the expectation value of $\cos^2\theta$, quantifying the early (nearly classical) and late (purely quantal) alignment enhancement stages. The dashed curve in the inset in (b) gives a generic weak field ($I = 10^8$ W cm^{-2}) rotational beat pattern [6], where we modified the initial condition to $J_i = 2$ in order to allow for more than a single rotational branch under perturbative conditions. The dotted curve corresponds to an intermediate intensity (5×10^9 W cm^{-2}) where (with $J_i = 2$) four rotational branches contribute to the excited state beat pattern but rotational excitation is intensity—rather than time—limited, as in the perturbative case.

We consider, for concreteness, the case of linearly polarized, near-resonance field and a parallel transition but the conclusions are general. At nonperturbative intensities sequential Rabi-type cycles, each accompanied by an exchange of one unit of angular momentum between the field and the molecule, excite coherent rotational wave packets of opposite parity in both electronic states while the space-fixed projection of the angular momentum is conserved. Assuming that the system is initially prepared in the ground rotational level the wave packet (in either electronic state) is given subsequent to the pulse as $\Psi(\theta, t) = \sum_J C^J P_J(\cos\theta) e^{-iB_e J(J+1)t}$, where P_J are Legendre polynomials and the rotational energies are approximated within a rigid rotor model, B_e being the rotational constant. Of interest for the study of alignment is the wave packet in the forward direction,

$$\Psi(\theta = 0, t) = \sum_{j=-\infty}^{\infty} C^{J_0 - 2j} \exp\left[2\pi i\left(\frac{t}{T_{\rm per}}\, j - \frac{2t}{T_{\rm rev}}\, j^2\right)\right], \tag{1}$$

where energy is measured with respect to the peak of the coefficients distribution J_0, and $2j = J_0 - J$. We noted that $P_J(1) = 1$ and denoted by $T_{\rm rev}$ the full revival time, $T_{\rm rev} = \pi/B_e$ [17]. $T_{\rm per} = \pi/B_e(2J_0 + 1)$ takes the role of a classical period, $2B_e(2J_0 + 1)$ being an average level spacing around J_0.

An analytical approximation for the coefficients C^J, applicable under nonperturbative intensities, is [1]

$$C^J \approx e^{-i\pi J/2}\, \frac{J + 1}{\zeta}\, J_{J+1}(2\zeta), \qquad \zeta = \Omega_R \int f(t)\, dt\,, \tag{2}$$

where J_J is a Bessel function, Ω_R is the Rabi coupling, and $f(t)$ is the pulse envelope. Equation (2) applies to the short pulse case, where "short" is to be taken in the sense that the degree of rotational excitation is upper bounded by the pulse duration, rather than by the requirement of sufficient intensity to compensate for the detuning from resonance (Δ^J). That is, $J_{\rm max} \sim \zeta$ and $\Omega_R > \Delta^{J_{\rm max}}$ [1]. Equation (2) notes a qualitative difference between strong-field-induced rotational wave packets and vibrational, or electronic wave packets, which can be produced with perturbative fields, with a consequent difference of their revival structures. In the latter cases the coefficient distribution can be modeled as a real Gaussian distribution [10], reflecting the laser pulse. In the former case C^J is an asymmetric, oscillatory function of J which carries an all important phase.

Using the Poisson summation formula, Eq. (1) can be cast in the form [10]

$$\Psi(0, t) = \sum_{m=-\infty}^{\infty} I[a_m(t), b(t)], \tag{3}$$

where $I(a, b) = \int dj\, C(j) \exp[2\pi i(aj - bj^2)]$, $a_m(t) = t/T_{\rm per} - m$, and $b(t) = 2t/T_{\rm rev}$. The advantage of Eq. (3) over the equivalent (1) will become clear below. Equation (2) does not allow analytical evaluation of $I(a, b)$. An accurate approximation for the coefficients, which lends itself to analytical manipulation and allows better insight into the excitation process, is given (up to a normalization factor) as

$$C(j) \simeq e^{i\pi(j - J_0/2)} \exp(-Aj^2 + Bj) \cos(\alpha j^2), \tag{4}$$

where A, B, α, and J_0 are determined by the effective coupling parameter ζ, containing the information about

the excitation dynamics. In practice they are obtained by a numerical fit of Eq. (2). For small ζ, the distribution is nearly Gaussian, centered about $J_0 \simeq 2\zeta - 1$ with variance $\Delta J = (2A)^{-\frac{1}{2}}$. As ζ increases the oscillation frequency at $j > 0$ increases and the asymmetry of the Gaussian is accentuated. For large coupling, like Eq. (2) and numerically determined coefficients for realistic systems, C^J of Eq. (4) are characterized by a rapid truncation at $J > J_0$ and a gradual, oscillatory turn-off at $J < J_0$.

With Eq. (4) $I(a, b)$ take the form

$$I[a_m(t), b(t)] = \frac{1}{2} e^{-i\pi J_0/2}\left[\frac{\pi^2}{\Delta_t^{\pm}}\right]^{1/4} \exp\left\{\frac{1}{\Delta_t^{\pm}}[-\overline{a}^2\pi^2 A + \overline{a}\pi B(2\pi b \pm \alpha) + B^2 A/4]\right\} \times \exp\left\{\frac{i}{\Delta_t^{\pm}}[\overline{a}^2\pi^2(2\pi b \pm \alpha) + \overline{a}\pi BA - B^2(2\pi b \pm \alpha)] + \frac{i}{2}\tan^{-1}\left(\frac{2\pi b \pm \alpha}{A}\right)\right\}, \quad (5)$$

where $\Delta_t^{\pm} \equiv A^2 + (2\pi b \pm \alpha)^2$, the signs are summed over and $\overline{a} = a + \frac{1}{2}$.

At short time, $2\pi b(t) \ll \alpha$, $I[a_m(t), b(t)]$ is a Fourier transform of the coefficients distribution. Direct correspondence between the time dependence of the $I[a_m(t), b(t)]$ and the j dependence of the coefficient distribution obtains also at long times: In the small ζ limit $I[a_m(t), b(t)]$ are essentially Gaussian, centered about $\overline{a}_m = 0$ with a time-dependent variance $\delta_t = \frac{2}{\pi} T_{\rm per}\sqrt{\frac{\Delta_t}{A}}$. As the Rabi coupling increases the asymmetry and the oscillations are accentuated and interference between sequential components sets in at an earlier time. In addition, with increasing coupling, J_0 increases and hence the period decreases and more components contribute.

Several features of Eq. (5) distinguish the postpulse evolution of strong-field-induced rotational wave packets from previously analyzed revival structures [10] and lead to the alignment enhancement after turn-off of the field observed in Fig. 1.

(i) At short times the $I[a_m(t), b(t)]$ do not interfere and maxima of the wave packet obtain at their centers, $t_m = (m - \frac{1}{2})T_{\rm per}$, $m = 1, \ldots,$. Mathematically it is thus a consequence of the phase of C^J, Eq. (2), that the first peak obtains not upon turn-off, as in the case of real coefficients, corresponding to weak field excitation of, e.g., electronic or vibrational wave packets [10], but rather half a period later. We note that, while the precise magnitude of the phase is a property of the present model, a nonzero, J-dependent phase of the C^J is general to strong-field-induced rotational wave packets.

(ii) At intermediate times, $t/T_{\rm rev} \gtrsim \alpha/2\pi$, such that $2\pi b$ is not negligible compared with α but the individual $I[a_m(t), b(t)]$ do not overlap, the preexponential, proportional to $t^{-1/2}$, diminishes the height of sequential m components in the Gaussian limit. In the asymmetric case, $B \neq 0$, the growing exponent $e^{\overline{a}B2\pi b}$ in Eq. (5), more than compensates for the effect of the preexponent and hence the wave-packet maxima increase with m.

(iii) At later times or stronger coupling constructive interference of sequential $I[a_m(t), b(t)]$ further enhances the maxima of $\Psi(t)$ as compared to the ones comprising a single m component. That such interference is constructive follows from the phase relationship between the wave-packet components: At its maximum amplitude, where $\overline{a}_m = 0$, the phase of $I[a_m(t), b(t)]$ has a local minimum and is positive definite. The phase of $I[a_{m-1}(t), b(t)]$ is a monotonically increasing (modulo 2π) function of time and intersects that of $I[a_m(t), b(t)]$ near its minimum. Overlap of the secondary peak of $I[a_{m-1}(t), b(t)]$ with the primary peak of $I[a_m(t), b(t)]$ allows the interference to produce a maximum in $\Psi(t)$. The same consideration therefore does not apply in the Gaussian limit. In the latter case sequential components interfere (constructively or destructively) only at time such that $\delta_t \sim T_{\rm per}$.

(iv) It follows from the highly nonlinear nature of rotational spectra that the revival time is very short. Thus, the long time $t \gg T_{\rm rev}$ evolution is characterized by a dense series of full revivals subsequent to each of which the alignment described in items (i)–(iii) is restored.

A question of formal and practical interest is the structure the wave packet takes at fractional revivals. A well-known feature of the quantum mechanical stage of the evolution of wave packets analyzed in the past is partitioning of the initially localized state into several spatially separated packets at each q/r fractional revival, $t \sim \frac{q}{r} T_{\rm rev}$, where q and r are mutually prime [9]. Such partitioning would imply destruction of the alignment between full revivals. This effect is neither observed in Fig. 1 nor predicted by the rigid rotor model since the classical limit of the aligned state is characterized by an extremely small classical orbit $L = 4\theta_m$, where $\theta_m \approx \tau\sqrt{B_e \Omega_R}$ is the amplitude of librational motion about the polarization axis. Consequently the fractions overlap in space, their width $\Delta\theta \sim 1/\Delta J$ exceeding the librational amplitude even in the nearly classical limit of large ΔJ. This qualitative argument is borne out by detailed analysis of Eq. (1) in the vicinity of arbitrary fractional revivals, to be described elsewhere.

It is worth reemphasizing that enhanced alignment obtains in the sudden excitation regime, to which Eq. (2) pertains [1]. By contrast, in the long pulse case [3], each eigenstate of the field-free Hamiltonian transforms adiabatically into the corresponding eigenstate of the full Hamiltonian (an aligned hybrid of many angular momenta levels) upon turn-on, returning to the field-free (isotropic)

state upon turn-off. Under these conditions alignment is lost once the interaction is over. With slow turn-on and sudden turn-off the adiabatically produced rotational hybrid is optimally phased upon turn-off and at each subsequent full revival. Thus, the alignment attained in the field is periodically reconstructed but not enhanced.

An average measure of the alignment is the expectation value of $\cos^2\theta$, shown as a solid curve in the insets in Fig. 1. The numerically computed $\langle\cos^2\theta\rangle$ for a complex rovibrational wave packet follows faithfully the evolution stages (i)–(iv) predicted within the rigid rotor approximation above. It continues to grow during the short-time, classical-like evolution immediately following the turn-off and is further enhanced at later times, where interference sets in. By contrast, with adiabatic turn-on and rapid turn-off of the interaction, $\langle\cos^2\theta\rangle$ reaches sharp maxima upon turn-off and at kT_{rev} but is otherwise close to $\frac{1}{3}$. The inset in Fig. 1(b) provides also a comparison of the strong-field-induced rotational revivals with the weak field rotational beat pattern [6] of Li_2 and with an intermediate intensity case.

While the revival structure can be precisely controlled through choice of the field parameters, the time-averaged alignment is only weakly dependent on the excitation coefficients. In the rigid rotor limit $\int dt\langle\cos^2\theta\rangle = \sum_j |C^J|^2(2J^2 + 2J - 1)/(4J^2 + 4J - 3) \sim \frac{1}{2}$. Time averaging washes out coherences, retaining only the alignment associated with the natural anisotropy of the wave-packet components.

To summarize, we studied numerically and analytically the revival structure of spatially aligned rotational wave packets, produced in nonperturbative near- or nonresonant laser fields through sequential, angular momentum nonconserving Rabi-type cycles. The analytical model exposes the physical origin of numerically observed significant alignment enhancement after turn-off of the field.

Spontaneous localization of a wave packet after turn-off of the interaction is a fascinating molecular property which may also carry practical benefits. Foremost, the possibility of preserving and enhancing the alignment under field-free conditions makes strong-field-induced rotational wave packets a potentially powerful tool for molecular alignment. Traditionally molecular alignment served for stereodynamical studies, gas-surface research, and surface catalysis, hence the long-standing search for general and efficient alignment techniques [11,12]. Recent work proposed the combination of alignment with focusing of the center-of-mass motion as a means of depositing orientationally ordered nanostructures on a substrate—potentially a route to new materials with predesigned electric and/or magnetic properties [13]. Clearly, both traditional and potential future applications rely on the possibility of aligning molecules under field-free conditions.

Possible extensions of the present work include optimization of the alignment using feedback control theory to tailor the excitation field, orientation through symmetry breaking, e.g., by use of two phase-related pulses, and "clocking" of predissociation reactions by tuning to resonance with a metastable state.

I am grateful to Dr. W. Siebrand, Dr. A. Stolow, and Dr. M. Yu. Ivanov for reading the manuscript and for making helpful comments.

*Electronic address: tamar.seideman@nrc.ca

[1] T. Seideman, J. Chem. Phys. **103**, 7887 (1995).
[2] B. Friedrich and D. R. Herschbach, Phys. Rev. Lett. **74**, 4623 (1995).
[3] W. Kim and P. M. Felker, J. Chem. Phys. **104**, 1147 (1996); H. Sakai, *et al.*, J. Chem. Phys. **110**, 10 235 (1999).
[4] J. A. Yeazell and C. R. Stroud, Jr., Phys. Rev. Lett. **60**, 1494 (1988).
[5] For a review, see, for instance, D. Zhong and A. H. Zewail, J. Phys. Chem. A **102**, 4031 (1998).
[6] It is important to distinguish the revival structure of rotationally broad, spatially well-defined wave packets from the beat pattern obtained in the weak field limit, where the components are trivially phased and subject to the standard spectroscopic selection rules. The weak field pattern has been extensively discussed in the framework of rotational coherence spectroscopy as a means of extracting rotational constants. For a review, see P. M. Felker, J. Phys. Chem. **96**, 7844 (1992).
[7] J. A. Yeazell and C. R. Stroud, Jr., Phys. Rev. A **43**, 5153 (1991).
[8] M. J. J. Vrakking, D. M. Villeneuve, and A. Stolow, Phys. Rev. A **54**, 37R (1996).
[9] I. Sh. Averbukh and N. F. Perel'man, Sov. Phys. JETP **69**, 464 (1989).
[10] C. Leichtle, I. Sh. Averbukh, and W. P. Schleich, Phys. Rev. Lett. **77**, 3999 (1996).
[11] For a review of various alignment techniques and their application in stereodynamical research, see B. Friedrich, D. P. Pullman, and D. R. Herschbach, J. Phys. Chem. **95**, 8118 (1991).
[12] V. A. Cho and R. B. Bernstein, J. Phys. Chem. **95**, 8129 (1991), and references therein.
[13] T. Seideman, Phys. Rev. A **56**, R17 (1997).
[14] A. Zavriyev *et al.*, Chem. Phys. Lett. **234**, 281 (1995).
[15] R. M. Williams *et al.*, J. Chem. Phys. **106**, 8299 (1997).
[16] R. B. Vrijen, G. M. Lankhuijzen, and L. D. Noordam, Phys. Rev. Lett. **79**, 617 (1997).
[17] The revival time is not given by the standard expression $T_{\mathrm{rev}} = \frac{4\pi}{d^2E_n/dn^2|n_0}$ [10] due to the parity property of rotational wave packets.